Frontiers of Information Technology & Electronic Engineering
www.jzus.zju.edu.cn; engineering.cae.cn; www.springerlink.com
ISSN 2095-9184 (print); ISSN 2095-9230 (online)
E-mail: jzus@zju.edu.cn

Adaptive tracking control of high-order MIMO nonlinear systems with prescribed performance*

Xuerao WANG[1,2], Qingling WANG[1,2], Changyin SUN‡[1,2]

[1]*School of Automation, Southeast University, Nanjing 210096, China*

[2]*Key Laboratory of Measurement and Control of Complex Systems of Engineering, Ministry of Education, Southeast University, Nanjing 210096, China*

E-mail: wangxuerao@seu.edu.cn; qlwang@seu.edu.cn; cysun@seu.edu.cn

Received Apr. 3, 2020; Revision accepted Oct. 15, 2020; Crosschecked June 8, 2021

Abstract: In this paper, an observer-based adaptive prescribed performance tracking control scheme is developed for a class of uncertain multi-input multi-output nonlinear systems with or without input saturation. A novel finite-time neural network disturbance observer is constructed to estimate the system uncertainties and external disturbances. To guarantee the prescribed performance, an error transformation is applied to transfer the time-varying constraints into a constant constraint. Then, by employing a barrier Lyapunov function and the backstepping technique, an observer-based tracking control strategy is presented. It is proven that using the proposed algorithm, all the closed-loop signals are bounded, and the tracking errors satisfy the predefined time-varying performance requirements. Finally, simulation results on a quadrotor system are given to illustrate the effectiveness of the proposed control scheme.

Key words: Adaptive tracking control; Prescribed performance; Input saturation; Disturbance observer; Neural network

https://doi.org/10.1631/FITEE.2000145 **CLC number:** TP273

1 Introduction

The tracking control of multi-input multi-output (MIMO) nonlinear systems has attracted a great deal of attention over the past few decades because it is common in practice. Many practical mechanical systems can be modeled by MIMO nonlinear systems, including two-wheeled robot systems, manipulator systems, and quadrotor systems (Lin XB et al., 2019a; Lin LG and Xin, 2020; Peng et al., 2020). However, the nonlinear characteristics always lead to poor performance such that many traditional linear control methods lose their effectiveness, which influences the system stability. To solve this problem, many advanced nonlinear control techniques have been developed. Adaptive neural network (NN) control schemes were adopted for MIMO nonlinear systems as a useful solution to increase the robustness of the systems (Wang XJ et al., 2018; Ouyang et al., 2019, 2020). In Tong et al. (2012), the backstepping recursive design technique and NN approximation method were used to achieve tracking control of pure-feedback uncertain MIMO nonlinear systems. By employing a barrier Lyapunov function (BLF), a backstepping design method was presented to achieve fault-tolerant tracking control of MIMO nonlinear systems in Jin (2018).

A nonlinear system is often accompanied by uncertainties and external disturbances, which seriously degrade the control performance (Zhao et al.,

‡ Corresponding author

* Project supported by the National Key R&D Program of China (No. 2018AAA0101400), the National Natural Science Foundation of China (Nos. 61921004 and 61973074), and the Natural Science Foundation of Jiangsu Province, China (No. BK20202006)

ORCID: Xuerao WANG, https://orcid.org/0000-0002-5693-7527; Changyin SUN, https://orcid.org/0000-0001-9269-334X

2020a; Liu J et al., 2021). Accurate models are difficult to obtain due to the complicated working environment (Lin XB et al., 2019b). In Liu H et al. (2017), a robust compensation method was presented to reduce the influence of uncertainties and external disturbances in a quadrotor system. An uncertainty and disturbance estimator (UDE) was developed to estimate the combined influence of disturbances and uncertainties through a filter in Ren et al. (2015). However, the frequency-domain analysis in the above methods prevents them from being directly applied to MIMO nonlinear systems. Aside from these approaches, a disturbance-observer-based control scheme has been proposed to estimate unknown disturbances (Guo L and Chen, 2005; Chen WH et al., 2015; Lin XB et al., 2019a), where the observer can be designed separately. Compared with other methods, the disturbance-observer-based method has led to more rigorous results in stability analysis based on the Lyapunov stability theory. In Chen M et al. (2013), a disturbance observer was designed to handle the disturbance term in the sliding-mode control design process for the MIMO nonlinear system. In Sun and Guo (2016), a disturbance observer was integrated with NN methods, which further improved the anti-disturbance capability of the system. Nevertheless, in the literature discussed above, the performance of the observer itself is ignored. Thus, it is essential to introduce finite-time results to ensure the convergence rate (Fu et al., 2017; Liu J et al., 2019, 2020). Hu et al. (2014) presented a second-order observer whose error could reach the origin in finite time. In Wang DD et al. (2018), a finite-time NN disturbance observer based on radial basis functions was proposed for a fourth-order nonlinear system. However, the sign function may cause the chattering phenomenon in input signals (Hu et al., 2014; Wang DD et al., 2018). Hence, a high-performance disturbance observer needs to be investigated further.

The aforementioned works focus mainly on guaranteeing the steady-state system property, but they overlook the transient property, which is equally important (Zhao et al., 2020b). To achieve better and more precise control performance, a concept called prescribed performance was presented by Bechlioulis and Rovithakis (2008). Prescribed performance has high requirements for the steady-state error, convergence rate, and maximum overshoot at the same time, which brings more difficulty to the control design. The key idea to solve prescribed performance problems is transforming the "constrained" system into an equivalent "unconstrained" system through the output error transformation given in Bechlioulis and Rovithakis (2009). Meanwhile, various error transformation methods have been proposed (Han and Lee, 2013; Sui et al., 2015; Bu, 2018). A smooth and strictly increasing function was introduced in Han and Lee (2013) as a transformed function to deal with the prescribed bounds. Bu (2018) developed an adaptive fuzzy control approach for a MIMO nonlinear system by transferring the constrained system through a tanh-type error transformation. It is worth noting that during the above transitions, the inverse function of the error transformation must be counted, which leads to computing problems. Another solution was given in Sui et al. (2015), which gave a new type of error transformation without fuzzy calculation. However, a question remains, that is, how to achieve prescribed performance tracking control of high-order MIMO nonlinear systems in the presence of uncertainties, disturbances, and input constraints.

To guarantee system performance, the control constraints (in particular, input saturation) are problems that cannot be ignored. In practical systems, the control input signals are always unable to reach the designed range due to the limited capacity of the actuator system (He et al., 2015a; Zheng and Feroskhan, 2017). Chen M et al. (2011) considered the non-symmetric input saturation in the tracking control of MIMO systems and handled it by designing an auxiliary system. In Zhou et al. (2014), the input saturation function was approximated by a smooth curve to tackle the constraint.

Motivated by the literature noted above, in this paper, an observer-based adaptive tracking control scheme is proposed for a class of high-order MIMO nonlinear systems with uncertainties and external disturbances. The main contributions are as follows:

1. We formulate and solve the tracking control problem with prescribed performance for high-order MIMO nonlinear systems, where the system uncertainties and external disturbances are also considered. To the best of our knowledge, this is the first time to address this problem. In this paper, the designed procedure is divided into two phases: disturbance attenuation and prescribed performance

tracking control.

2. A novel NN disturbance observer is presented to handle the system uncertainties and external disturbances for high control performance. First, compared with the existing disturbance observers for MIMO nonlinear systems in Chen WH et al. (2015) and Sun and Guo (2016), the convergence time of the proposed observer is proven to be limited. Moreover, compared to the previous results (Hu et al., 2014; Wang DD et al., 2018), a continuous signal in the finite-time observer is achieved to avoid chattering problems.

3. The control scheme is developed using the BLF and the backstepping technique. With the error transformation, a new solution is given to guarantee the predefined tracking performance for high-order MIMO nonlinear systems. Furthermore, the input saturation is considered as an extension.

2 Problem formulation and preliminaries

2.1 System description

Consider the following high-order MIMO nonlinear system:

$$\begin{cases} \dot{\boldsymbol{x}}_i = \boldsymbol{x}_{i+1} + \boldsymbol{f}_i(\boldsymbol{x}_i) + \Delta\boldsymbol{f}_i(\boldsymbol{x}_i) + \boldsymbol{d}_i(t), \\ \dot{\boldsymbol{x}}_n = \boldsymbol{b}\boldsymbol{u} + \boldsymbol{f}_n(\boldsymbol{x}_n) + \Delta\boldsymbol{f}_n(\boldsymbol{x}_n) + \boldsymbol{d}_n(t), \\ \boldsymbol{y} = \boldsymbol{x}_1, \end{cases} \tag{1}$$

where $\boldsymbol{x}_i = [x_{i1},\ x_{i2},\ \ldots,\ x_{im}]^{\mathrm{T}} \in \mathbb{R}^m$ (i=1, 2, ..., n) denotes the state vector of the i^{th} system, $\boldsymbol{y} = [y_1, y_2, ..., y_m]^{\mathrm{T}} \in \mathbb{R}^m$ denotes the output vector of the overall system, $\boldsymbol{u} \in \mathbb{R}^m$ denotes the control input vector, $\boldsymbol{b} \in \mathbb{R}^{m\times m}$ is the known control coefficient matrix (supposed to be nonsingular and its Frobenius norm is bounded), $\boldsymbol{f}_i(\cdot) : \mathbb{R}^m \to \mathbb{R}^m$ (i=1, 2, ..., n) is a known smooth nonlinear function denoting the acquirable part of the system, $\Delta\boldsymbol{f}_i(\boldsymbol{x}_i)$ is an unknown smooth function representing the system uncertainties composed of unmodeled dynamics and parametric uncertainties, and $\boldsymbol{d}_i(t) \in \mathbb{R}^m$ (i=1, 2, ..., n) is the time-varying external disturbance. In addition, we define $\boldsymbol{X} = [\boldsymbol{x}_1^{\mathrm{T}},\ \boldsymbol{x}_2^{\mathrm{T}},\ ...,\ \boldsymbol{x}_n^{\mathrm{T}}]^{\mathrm{T}}$ as a measurable state vector.

According to Guo XX et al. (2019), matrix $\boldsymbol{b}$ could be divided into a symmetric matrix $\boldsymbol{b}_1$ and a skew-symmetric matrix $\boldsymbol{b}_2$. Then, $\dot{\boldsymbol{x}}_n$ in Eq. (1) can be rewritten as

$$\dot{\boldsymbol{x}}_n = \boldsymbol{b}_1\boldsymbol{u} + \boldsymbol{b}_2\boldsymbol{u} + \boldsymbol{f}_n(\boldsymbol{x}_n) + \Delta\boldsymbol{f}_n(\boldsymbol{x}_n) + \boldsymbol{d}_n(t), \tag{2}$$

where $\boldsymbol{b}_1 = \frac{1}{2}(\boldsymbol{b}+\boldsymbol{b}^{\mathrm{T}})$ and $\boldsymbol{b}_2 = \frac{1}{2}(\boldsymbol{b}-\boldsymbol{b}^{\mathrm{T}})$. Obviously, $\boldsymbol{b}_1$ is also a nonsingular matrix and its Frobenius norm is bounded.

The control objective is to drive the output $\boldsymbol{y}$ to follow the given desired trajectory $\boldsymbol{y}_{\mathrm{d}}$, while the tracking error $\boldsymbol{e} = \boldsymbol{y}(t) - \boldsymbol{y}_{\mathrm{d}}(t)$ can guarantee the prescribed performance. In addition, all closed-loop signals are ensured to be bounded.

Without loss of generality, we give some assumptions as follows:

Assumption 1 (Fan et al., 2017) The system uncertainty $\boldsymbol{\Delta}_i(\boldsymbol{x}_i, t)$ is bounded and satisfies $\|\boldsymbol{\Delta}_i(\boldsymbol{x}_i, t)\| \le \Delta_m$, where Δ_m is an unknown positive constant.

Assumption 2 (Wang CC and Yang, 2018) The unknown disturbance $\boldsymbol{d}_i(t)$ is bounded with a positive constant d_m, which satisfies $\|\boldsymbol{d}_i(t)\| \le d_m$.

Assumption 3 (Song et al., 2017) The desired trajectory vector $\boldsymbol{y}_{\mathrm{d}}(t)$ and its derivatives up to the $(n-1)^{\mathrm{th}}$ order are continuous and bounded.

2.2 Mathematical preliminaries

In this subsection, several useful lemmas and an important definition are revisited.

Lemma 1 (Wang LY et al., 2009) Given any positive numbers a_1, a_2, ..., a_n and $0 < p < 1$, the following inequality holds:

$$(a_1^2 + a_2^2 + ... + a_n^2)^{2p} \le (a_1^{2p} + a_2^{2p} + ... + a_n^{2p})^2. \tag{3}$$

Lemma 2 (He et al., 2015b) For any positive vector $\boldsymbol{k} \in \mathbb{R}^n$, the following inequality holds for any vector $\boldsymbol{x} \in \mathbb{R}^n$ which satisfies $\|\boldsymbol{x}\| < \|\boldsymbol{k}\|$:

$$\ln \frac{\boldsymbol{k}^{\mathrm{T}}\boldsymbol{k}}{\boldsymbol{k}^{\mathrm{T}}\boldsymbol{k} - \boldsymbol{x}^{\mathrm{T}}\boldsymbol{x}} \le \frac{\boldsymbol{x}^{\mathrm{T}}\boldsymbol{x}}{\boldsymbol{k}^{\mathrm{T}}\boldsymbol{k} - \boldsymbol{x}^{\mathrm{T}}\boldsymbol{x}}. \tag{4}$$

Lemma 3 (Zhu et al., 2011) For the following system $\dot{\boldsymbol{x}} = \boldsymbol{f}(\boldsymbol{x},\ \boldsymbol{u})$, where $\boldsymbol{x}$ is the system state vector and $\boldsymbol{u}$ is the control input, we say the system is practical finite-time stable (PFS) if for any initial state $\boldsymbol{x}(0)$, there exist $\epsilon > 0$ and $T_{\mathrm{f}}(\epsilon,\ \boldsymbol{x}_0) < \infty$, such that $\|\boldsymbol{x}(t)\| < \epsilon$, for all $t \ge t_0 + T_{\mathrm{f}}$. Then we have a continuous Lyapunov function $V(\boldsymbol{x})$ and its derivative satisfies:

$$\dot{V}(\boldsymbol{x}) \le -\rho V^{\alpha}(\boldsymbol{x}) + b, \tag{5}$$

where $\rho > 0$, $0 < \alpha < 1$, and $0 < b < \infty$. Moreover, $0 < \tau < 1$ is given so that the system state can be bounded in finite time as

$$\lim_{\tau \to \theta_0} \boldsymbol{x} \in \left(V^{\alpha}(\boldsymbol{x}) \leq \frac{b}{(1-\tau)\rho} \right), \tag{6}$$

where $0 < \theta_0 < 1$, and the maximum convergence time to reach Eq. (6) is given as

$$T \leq \frac{V^{1-\alpha}(\boldsymbol{x}_0)}{\rho\theta_0(1-\alpha)}. \tag{7}$$

Lemma 4 (He et al., 2015b) Consider a positive definite and continuous Lyapunov function $V(\boldsymbol{x})$. In case its initial condition $V(\boldsymbol{0})$ is bounded and the following inequality is satisfied:

$$\dot{V}(\boldsymbol{x}) \leq -aV(\boldsymbol{x}) + b, \tag{8}$$

where $a > 0$ and $b > 0$, then $V(\boldsymbol{x})$ is bounded.

Definition 1 (Tee et al., 2009) A barrier Lyapunov function $V(\boldsymbol{x})$ is a continuous, positive definite, scalar function, which is defined on an open region Ω including the origin, relating to the system $\dot{\boldsymbol{x}} = \boldsymbol{f}(\boldsymbol{x})$. At each point of Ω, the first-order partial derivatives of the BLF are continuous. When $\boldsymbol{x}$ gets close to the margin of Ω, there is $V(\boldsymbol{x}) \to \infty$. Besides, along the solution of $\dot{\boldsymbol{x}} = \boldsymbol{f}(\boldsymbol{x})$, there is $V(\boldsymbol{x}(t)) \leq q$ $(\forall t \geq 0)$ with a positive constant q.

2.3 Prescribed performance

The present control objective establishes the requirement for the output of the whole system with a guaranteed prescribed performance.

Definition 2 (Bechlioulis and Rovithakis, 2010) The performance function $\rho : \mathbb{R}_+ \to \mathbb{R}_+$ is a smooth function which satisfies the requirements as follows:

(1) $\rho(t)$ is positive and decreasing;

(2) $\lim_{t \to \infty} \rho(t) = \rho_\infty > 0$.

In this study, the performance function is chosen as $\rho_i(t) = (\rho_{i0} - \rho_{i\infty})\mathrm{e}^{l_i t} + \rho_{i\infty}$, where the performance parameters ρ_{i0}, $\rho_{i\infty}$, and l_i are given to ensure the behavior of the traces. Based on the performance function, the tracking errors are confined within the preset region, which can be described as

$$-\sigma_{i1}\rho_{i1}(t) < \mathrm{sign}(e_{i0}) \cdot e_i < \sigma_{i2}\rho_{i2}(t),\ i = 1, 2, ..., n, \tag{9}$$

where σ_{i1} and σ_{i2} are positive constants designed to adjust the error boundaries and overshoots. In general, σ_{i1} should be taken smaller than σ_{i2} for less overshoot. The sign of initial error e_{i0} is taken into account to adjust the predefined range.

Remark 1 Compared with the previous schemes in which the sign of e_{i0} is overlooked, the condition given in inequality (9) can adjust the location of the upper and lower bounds according to the initial error. Compared to the boundaries given in Bechlioulis and Rovithakis (2010), the upper and lower bounds in inequality (9) are allowed to set different values separately to adapt to various control requirements.

3 Main results

3.1 Finite-time neural network disturbance observer design

In this study, the radial basis function (RBF) NN is chosen to construct an NN observer for disturbance estimation. For a continuous function $\boldsymbol{q}(\boldsymbol{x})$ in a compact set $\Omega_{\boldsymbol{q}}$, we have an NN estimator as

$$\boldsymbol{q}(\boldsymbol{x}) = (\boldsymbol{W}^*)^{\mathrm{T}} \boldsymbol{S}(\boldsymbol{x}) + \boldsymbol{\epsilon}(\boldsymbol{x}), \tag{10}$$

where the input vector $\boldsymbol{x} \in \Omega_{\boldsymbol{q}} \subset \mathbb{R}^n$, $\boldsymbol{W}^*$ is the optimal weight matrix of the network which could minimize the approximation error $\boldsymbol{\epsilon}(\boldsymbol{x})$, and $\boldsymbol{\epsilon}(\boldsymbol{x})$ satisfies $\|\boldsymbol{\epsilon}(\boldsymbol{x})\| \leq \overline{\epsilon}$ with $\overline{\epsilon}$ being an unknown positive constant. The actual weight matrix is denoted as $\hat{\boldsymbol{W}}$, and the weight error is denoted as $\widetilde{\boldsymbol{W}} = \boldsymbol{W}^* - \hat{\boldsymbol{W}}$. $\boldsymbol{S}(\boldsymbol{x}) = [S_1(\boldsymbol{x}),\ S_2(\boldsymbol{x}),\ ...,\ S_m(\boldsymbol{x})]^{\mathrm{T}}$ is the activation function vector whose terms can be described as

$$S_i(\boldsymbol{x}) = \exp\left[\frac{-(\boldsymbol{x} - \boldsymbol{c}_j)^{\mathrm{T}}(\boldsymbol{x} - \boldsymbol{c}_j)}{b_j^2} \right], \tag{11}$$

where $i = 1, 2, ..., m,\ j = 1, 2, ..., k$, and $\boldsymbol{c}_j$ and b_j are the j^{th} center value and width value of the i^{th} neuron, respectively.

In system (1), the uncertainties and external disturbances can be regarded as single equivalent disturbances, which is common in disturbance observer design (Chen WH, 2004; Chen XS et al., 2009; Chen WH et al., 2015). Therefore, a total disturbance term for ease of observation is given as

$$\boldsymbol{\Delta}_i(t) = \Delta \boldsymbol{f}_i(\boldsymbol{x}_i) + \boldsymbol{d}_i(t),\ i = 1,\ 2,\ ...,\ n. \tag{12}$$

According to the above principles of an RBF NN, the estimation results of the total disturbance term can be obtained:

$$\begin{aligned} \boldsymbol{\Delta}_i(t) &= (\boldsymbol{W}_i^*)^{\mathrm{T}} S_i(\boldsymbol{\varsigma}_i) + \boldsymbol{\epsilon}_i(\boldsymbol{\varsigma}_i) \\ &= \hat{\boldsymbol{W}}_i^{\mathrm{T}} S_i(\boldsymbol{\varsigma}_i) + \widetilde{\boldsymbol{W}}_i^{\mathrm{T}} S_i(\boldsymbol{\varsigma}_i) + \boldsymbol{\epsilon}_i(\boldsymbol{\varsigma}_i), \end{aligned} \tag{13}$$

where $\boldsymbol{\varsigma}_i \in \mathbb{R}^m$ is the input vector which contains the state $\boldsymbol{x}_i$ and its derivative $\dot{\boldsymbol{x}}_i$, and $\boldsymbol{\epsilon}_i(\boldsymbol{\varsigma}_i) \in \mathbb{R}^m$ is the estimation error vector which satisfies $\|\boldsymbol{\epsilon}_i(\boldsymbol{\varsigma}_i)\| \leq \overline{\epsilon}_i$ with $\overline{\epsilon}_i$ being an unknown positive constant.

An auxiliary variable is introduced as $\boldsymbol{s}_i = \boldsymbol{x}_i - \hat{\boldsymbol{x}}_i$. Then the NN disturbance observer is designed as

$$\begin{cases} \dot{\hat{\boldsymbol{x}}}_i = \boldsymbol{x}_{i+1} + \boldsymbol{f}_i(\boldsymbol{x}_i) + \hat{\boldsymbol{\Delta}}_i, \\ \dot{\hat{\boldsymbol{x}}}_n = \boldsymbol{b}\boldsymbol{u} + \boldsymbol{f}_n(\boldsymbol{x}_n) + \hat{\boldsymbol{\Delta}}_n, \\ \hat{\boldsymbol{\Delta}}_i = \hat{\boldsymbol{W}}_i^{\mathrm{T}} S_i(\boldsymbol{\varsigma}_i) + \tanh(\boldsymbol{s}_i/\vartheta)\nu_i + \boldsymbol{k}_{0i}\boldsymbol{s}_i^{\alpha_i}, \end{cases} \tag{14}$$

where $\hat{\boldsymbol{x}}_i \in \mathbb{R}^m$ and $\hat{\boldsymbol{\Delta}}_i \in \mathbb{R}^m$ (i=1, 2, ..., n) are the estimates of $\boldsymbol{x}_i$ and $\boldsymbol{\Delta}_i$ respectively, ϑ is defined as $\vartheta = 1/(1+t^2)$, ν_i is a constant selected to satisfy $\nu_i \geq \overline{\epsilon}_i$, $\boldsymbol{k}_{0i}$ is the designed positive constant parameter, and α_i is defined as $0 < \alpha_i = a_i/b_i$ with a_i and b_i being positive odd integers and satisfying $a_i < b_i$.

Considering observer (14), the time derivative of $\boldsymbol{s}_i$ can be written as

$$\begin{aligned} \dot{\boldsymbol{s}}_i &= \dot{\boldsymbol{x}}_i - \dot{\hat{\boldsymbol{x}}}_i = \boldsymbol{\Delta}_i - \hat{\boldsymbol{\Delta}}_i \\ &= \widetilde{\boldsymbol{W}}_i^{\mathrm{T}} S_i(\boldsymbol{\varsigma}_i) + \boldsymbol{\epsilon}_i(\boldsymbol{\varsigma}_i) - \tanh(\boldsymbol{s}_i/\vartheta)\nu_i - \boldsymbol{k}_{0i}\boldsymbol{s}_i^{\alpha_i}. \end{aligned} \tag{15}$$

The adaptive law for updating networks is designed as

$$\dot{\hat{\boldsymbol{W}}}_i = \boldsymbol{\Gamma}_i(S_i(\boldsymbol{\varsigma}_i)\boldsymbol{s}_i^{\mathrm{T}} + \kappa_i\hat{\boldsymbol{W}}_i), \tag{16}$$

where $\boldsymbol{\Gamma}_i$ is the learning rate matrix of NNs and will be designed later, and κ_i is a small positive constant.

With the above analysis, we can present the following theorem:

Theorem 1 Consider the high-order MIMO nonlinear system (1), if the NN disturbance observer (14) is used to estimate the total disturbance with the adaptive law (16), the estimation errors $\boldsymbol{s}_i$ will converge to a very small neighborhood of the origin in finite time.

Proof Consider a Lyapunov function candidate as

$$V_{i0} = \frac{1}{2}\boldsymbol{s}_i^{\mathrm{T}}\boldsymbol{s}_i + \frac{1}{2}\mathrm{tr}(\widetilde{\boldsymbol{W}}_i^{\mathrm{T}}\boldsymbol{\Gamma}_i^{-1}\widetilde{\boldsymbol{W}}_i), \tag{17}$$

where $\mathrm{tr}(\cdot)$ is the trace of the matrix. Substituting Eq. (15) and the designed adaptive law (16) into Eq. (17) results in

$$\begin{aligned} \dot{V}_{i0} =& \boldsymbol{s}_i^{\mathrm{T}}\dot{\boldsymbol{s}}_i + \mathrm{tr}(\widetilde{\boldsymbol{W}}_i^{\mathrm{T}}\boldsymbol{\Gamma}_i^{-1}\dot{\widetilde{\boldsymbol{W}}}_i) \\ =& \boldsymbol{s}_i^{\mathrm{T}}(\widetilde{\boldsymbol{W}}_i^{\mathrm{T}} S_i(\boldsymbol{\varsigma}_i) + \boldsymbol{\epsilon}_i(\boldsymbol{\varsigma}_i) - \tanh(\boldsymbol{s}_i/\vartheta)\nu_i - \boldsymbol{k}_{0i}\boldsymbol{s}_i^{\alpha_i}) \\ &+ \mathrm{tr}(\widetilde{\boldsymbol{W}}_i^{\mathrm{T}}\boldsymbol{\Gamma}_i^{-1}\dot{\widetilde{\boldsymbol{W}}}_i) \\ =& \boldsymbol{s}_i^{\mathrm{T}}\boldsymbol{\epsilon}_i(\boldsymbol{\varsigma}_i) - \boldsymbol{s}_i^{\mathrm{T}}\tanh(\boldsymbol{s}_i/\vartheta)\nu_i - \boldsymbol{s}_i^{\mathrm{T}}\boldsymbol{k}_{0i}\boldsymbol{s}_i^{\alpha_i} \\ &+ \mathrm{tr}(\widetilde{\boldsymbol{W}}_i^{\mathrm{T}}(\boldsymbol{\Gamma}_i^{-1}\dot{\widetilde{\boldsymbol{W}}}_i + S_i(\boldsymbol{\varsigma}_i)\boldsymbol{s}_i^{\mathrm{T}})) \\ =& \boldsymbol{s}_i^{\mathrm{T}}\boldsymbol{\epsilon}_i - \boldsymbol{s}_i^{\mathrm{T}}\tanh(\boldsymbol{s}_i/\vartheta)\nu_i - \boldsymbol{s}_i^{\mathrm{T}}\boldsymbol{k}_{0i}\boldsymbol{s}_i^{\alpha_i} \\ &+ \kappa_i\mathrm{tr}(\widetilde{\boldsymbol{W}}_i^{\mathrm{T}}\hat{\boldsymbol{W}}_i). \end{aligned} \tag{18}$$

Using the inequalities $|s_{ij}| - s_{ij}\cdot\tanh(s_{ij}/\vartheta) \leq 0.2785\vartheta$ (where s_{ij} (j=1, 2, ..., m) is the j^{th} element of $\boldsymbol{s}_i$) given in Wang QL and Sun (2020) and $\nu_i \geq \overline{\epsilon}_i$, we can derive

$$\begin{aligned} \boldsymbol{s}_i^{\mathrm{T}}\boldsymbol{\epsilon}_i - \boldsymbol{s}_i^{\mathrm{T}}\tanh(\boldsymbol{s}_i/\vartheta)\nu_i &\leq \|\boldsymbol{s}_i\|\overline{\epsilon}_i - \boldsymbol{s}_i^{\mathrm{T}}\tanh(\boldsymbol{s}_i/\vartheta)\nu_i \\ &\leq \|\boldsymbol{s}_i\|\overline{\epsilon}_i - \boldsymbol{s}_i^{\mathrm{T}}\tanh(\boldsymbol{s}_i/\vartheta)\overline{\epsilon}_i \\ &\leq 0.2785m\vartheta\overline{\epsilon}_i. \end{aligned} \tag{19}$$

Therefore, using Eq. (18), inequality (19), and Young's inequality, we can obtain

$$\begin{aligned} \dot{V}_{i0} \leq& -\boldsymbol{s}_i^{\mathrm{T}}\boldsymbol{k}_{0i}\boldsymbol{s}_i^{\alpha_i} + 0.2785\vartheta\overline{\epsilon}_i + \kappa_i\mathrm{tr}(\widetilde{\boldsymbol{W}}_i^{\mathrm{T}}\boldsymbol{W}_i^* - \widetilde{\boldsymbol{W}}_i^{\mathrm{T}}\widetilde{\boldsymbol{W}}_i) \\ \leq& -\lambda_{\min}(\boldsymbol{k}_{0i})\sum_{i=1}^{n}\boldsymbol{s}_i^{\alpha_i+1} + 0.2785m\vartheta\overline{\epsilon}_i \\ &+ \kappa_i\mathrm{tr}\left(\left(\frac{1}{2\sigma} - 1\right)\widetilde{\boldsymbol{W}}_i^{\mathrm{T}}\widetilde{\boldsymbol{W}}_i + \frac{\sigma}{2}\left(\boldsymbol{W}_i^*\right)^{\mathrm{T}}\boldsymbol{W}_i^*\right) \\ \leq& -\lambda_{\min}(\boldsymbol{k}_{0i})\sum_{i=1}^{n}\boldsymbol{s}_i^{\alpha_i+1} + 0.2785m\vartheta\overline{\epsilon}_i \\ &- \frac{\kappa_i(2\sigma-1)}{2\sigma}\mathrm{tr}(\widetilde{\boldsymbol{W}}_i^{\mathrm{T}}\widetilde{\boldsymbol{W}}_i) + \frac{\kappa_i\sigma}{2}\mathrm{tr}\left(\left(\boldsymbol{W}_i^*\right)^{\mathrm{T}}\boldsymbol{W}_i^*\right) \\ \leq& -\lambda_{\min}(\boldsymbol{k}_{0i})\sum_{i=1}^{n}\boldsymbol{s}_i^{\alpha_i+1} + 0.2785m\vartheta\overline{\epsilon}_i \\ &- \frac{\kappa_i(2\sigma-1)}{2\sigma}\mathrm{tr}(\widetilde{\boldsymbol{W}}_i^{\mathrm{T}}\widetilde{\boldsymbol{W}}_i) + \frac{\kappa_i\sigma}{2}\mathrm{tr}\left(\left(\boldsymbol{W}_i^*\right)^{\mathrm{T}}\boldsymbol{W}_i^*\right) \\ &+ \frac{\kappa_i(2\sigma-1)}{2\sigma}\left(\mathrm{tr}(\widetilde{\boldsymbol{W}}_i^{\mathrm{T}}\widetilde{\boldsymbol{W}}_i)\right)^{\frac{a+b}{2b}} \\ &- \frac{\kappa_i(2\sigma-1)}{2\sigma}\left(\mathrm{tr}(\widetilde{\boldsymbol{W}}_i^{\mathrm{T}}\widetilde{\boldsymbol{W}}_i)\right)^{\frac{a+b}{2b}} \\ \leq& -\lambda_{\min}(\boldsymbol{k}_{0i})\sum_{i=1}^{n}\boldsymbol{s}_i^{\alpha_i+1} + \frac{\beta_i\sigma}{2}\mathrm{tr}\left(\left(\boldsymbol{W}_i^*\right)^{\mathrm{T}}\boldsymbol{W}_i^*\right) \\ &+ 0.2785\vartheta\overline{\epsilon}_i - \frac{\kappa_i(2\sigma-1)}{2\sigma}\left(\mathrm{tr}(\widetilde{\boldsymbol{W}}_i^{\mathrm{T}}\widetilde{\boldsymbol{W}}_i)\right)^{\frac{a+b}{2b}} \\ \leq& -\lambda_{\min}(\boldsymbol{k}_{0i})2^{\frac{a+b}{2b}}\left(\frac{1}{2}\boldsymbol{s}_i^{\mathrm{T}}\boldsymbol{s}_i\right)^{\frac{a+b}{2b}} + 0.2785m\vartheta\overline{\epsilon}_i \\ &- \lambda_{\min}(\boldsymbol{k}_{0i})2^{\frac{a+b}{2b}}\frac{1}{2}\left(\mathrm{tr}(\widetilde{\boldsymbol{W}}_i^{\mathrm{T}}\boldsymbol{\Gamma}_i^{-1}\widetilde{\boldsymbol{W}}_i)\right)^{\frac{a+b}{2b}} \\ &+ \frac{\kappa_i\sigma}{2}\mathrm{tr}\left(\left(\boldsymbol{W}_i^*\right)^{\mathrm{T}}\boldsymbol{W}_i^*\right) \\ \leq& -\lambda_{\min}(\boldsymbol{k}_{0i})2^{\frac{a+b}{2b}}V_{i0}^{\frac{a+b}{2b}} + \eta_i, \end{aligned} \tag{20}$$

where $\lambda_{\min}(\cdot)$ represents the minimum eigenvalue of the vector, σ is a positive real number, and the

parameters are given by

$$\begin{cases} \boldsymbol{\Gamma}_i = \dfrac{2\sigma}{\kappa_i(2\sigma-1)}\boldsymbol{k}_{0i}, \\ \eta_i = 0.2785m\vartheta\overline{\epsilon}_i + \dfrac{\kappa_i\sigma}{2}\mathrm{tr}\left(\left(\boldsymbol{W}_i^*\right)^{\mathrm{T}}\boldsymbol{W}_i^*\right). \end{cases} \tag{21}$$

According to Lemma 3, the observer estimation errors $\boldsymbol{s}_i$ will be bounded in finite time, and can be calculated as

$$\lim_{\theta\to\theta_0}\boldsymbol{s}_i \in \left(V_{i0}^{\frac{a+b}{2b}} \le \frac{\eta_i}{(1-\theta)\lambda_{\min}(\boldsymbol{k}_{0i})2^{\frac{a+b}{2b}}}\right), \tag{22}$$

where $0<\theta\le 1$ and $0<\theta_0<1$. The convergence time is bounded as

$$T_i \le 2^{-\frac{a+b}{2b}}\cdot\frac{\left(V_{i0}(\boldsymbol{s}_{i0})\right)^{\frac{b-a}{2b}}}{\frac{b-a}{2b}\theta_0\lambda_{\min}(\boldsymbol{k}_{0i})}, \tag{23}$$

where $V_{i0}(\boldsymbol{s}_{i0})$ is the initial value of V_{i0}. This completes the proof.

Remark 2 The observer's performance is often ignored in previous works. As an important part of the integrated controller, the convergence time of the observer will influence the overall system performance. Compared with previous results (e.g., Guo L and Chen (2005), Chen M et al. (2013), Chen WH et al. (2015), and Sun and Guo (2016)), in this study, the proposed observer is proven to converge in finite time. Instead of using the signal functions in Hu et al. (2014) and Wang DD et al. (2018), the tanh function is chosen to construct the observer. In this way, the chattering phenomenon will be eliminated. Moreover, the disturbance observer design is separated from the controller design, and remains flexible to integrate with other control laws.

3.2 Tracking error transformation

To achieve the prescribed performance given in Section 2.3, the original system will be transformed by an error transformation function.

For simplicity, the condition given in inequality (9) is rewritten as

$$\chi_{i1}(t) < e_i < \chi_{i2}(t),\ i=1,\ 2,\ \ldots\ m, \tag{24}$$

where χ_{i1} and χ_{i2} are the lower and upper bounds of the tracking error associated with e_{i0}, respectively:

$$\begin{cases} \chi_{i1}(t) = \begin{cases} -\sigma_{i1}\rho_{i1}(t), & \text{if } e_{i0}\ge 0, \\ -\sigma_{i2}\rho_{i2}(t), & \text{if } e_{i0}<0, \end{cases} \\ \chi_{i2}(t) = \begin{cases} \sigma_{i2}\rho_{i2}(t), & \text{if } e_{i0}\ge 0, \\ \sigma_{i1}\rho_{i1}(t), & \text{if } e_{i0}<0. \end{cases} \end{cases} \tag{25}$$

Similar to Hu et al. (2017), the error transformation function is designed as

$$z_{1i}(t) = \frac{2e_i(t)-(\chi_{i1}(t)+\chi_{i2}(t))}{\chi_{i2}(t)-\chi_{i1}(t)}, \tag{26}$$

where i=1, 2, ..., m, and $z_{1i}(t)$ indicates the i^{th} element of the converted tracking error $\boldsymbol{z}_1$. With Eq. (26), the prescribed bounds (24) can be guaranteed by keeping the condition:

$$|z_{1i}(t)| < 1. \tag{27}$$

By differentiating Eq. (26), we can obtain

$$\dot{z}_{1i}(t) = \frac{2\dot{e}_i(t)}{\chi_{i2}(t)-\chi_{i1}(t)} - \iota_i(t), \tag{28}$$

where

$$\iota_i = \frac{\dot{\chi}_{i1}+\dot{\chi}_{i2}}{\chi_{i2}-\chi_{i1}} + \frac{[2e_i-(\chi_{i1}+\chi_{i2})](\dot{\chi}_{i2}-\dot{\chi}_{i1})}{(\chi_{i2}-\chi_{i1})^2}. \tag{29}$$

Then the transformed error dynamics coordinates of the original system (1) are defined as

$$\begin{cases} \dot{\boldsymbol{z}}_1 = [\dot{z}_{11}, \dot{z}_{12}..., \dot{z}_{1m}]^{\mathrm{T}} \\ \quad = \mathrm{diag}\left(\frac{2}{\chi_{i2}-\chi_{i1}}\right)(\boldsymbol{x}_2 + \boldsymbol{f}_1 + \boldsymbol{\Delta}_1 - \dot{\boldsymbol{y}}_{\mathrm{d}}) - \iota_i, \\ \dot{\boldsymbol{z}}_j = \boldsymbol{x}_{j+1} + \boldsymbol{f}_j(\boldsymbol{x}_j) + \Delta\boldsymbol{f}_j(\boldsymbol{x}_j) + \boldsymbol{d}_j(t) - \dot{\boldsymbol{\alpha}}_{j-1}, \\ \dot{\boldsymbol{z}}_n = \boldsymbol{b}\boldsymbol{u} + \boldsymbol{f}_n(\boldsymbol{x}_n) + \Delta\boldsymbol{f}_n(\boldsymbol{x}_n) + \boldsymbol{d}_n(t) - \dot{\boldsymbol{\alpha}}_{n-1}, \\ e_i = y_i - y_{\mathrm{d}i} = \frac{1}{2}z_{1i}(\chi_{i2}-\chi_{i1}) + (\chi_{i1}+\chi_{i2}), \end{cases} \tag{30}$$

where i=1, 2, ..., m, j=2, 3, ..., $n-1$, and $\boldsymbol{\alpha}_k$ (k=1, 2, ..., $n-1$) is the virtual control function.

3.3 Controller design and stability analysis

In Section 3.1, the finite-time NN disturbance observer has been developed to estimate and compensate for the lumped disturbance in the systems. On that basis, a barrier Lyapunov-based backstepping controller is designed to realize the proposed control objective.

Step 1: Define a Lyapunov function candidate that satisfies Definition 1:

$$V_1 = \frac{1}{2}\sum_{i=1}^{m}\ln\frac{1}{1-z_{1i}^2}. \tag{31}$$

According to Eq. (30), the time derivative of

Eq. (31) is given as

$$\begin{aligned}\dot{V}_1 &= \sum_{i=1}^{m}\frac{z_{1i}\dot{z}_{1i}}{1-z_{1i}^2}\\ &= \sum_{i=1}^{m}\frac{z_{1i}\left[\frac{2}{\chi_{i2}-\chi_{i1}}\cdot(x_{2i}+f_{1i}+\Delta_{1i}-\dot{y}_{\mathrm{d}i})-\iota_i\right]}{1-z_{1i}^2}\\ &= \sum_{i=1}^{m}\frac{z_{1i}\left[\frac{2}{\chi_{i2}-\chi_{i1}}\cdot(z_{2i}+\alpha_{1i}+f_{1i}+\Delta_{1i}-\dot{y}_{\mathrm{d}i})\right]}{1-z_{1i}^2}\\ &\quad-\sum_{i=1}^{m}\frac{-\iota_i}{1-z_{1i}^2}.\end{aligned} \tag{32}$$

The virtual control function α_{1i} is designed as

$$\begin{aligned}\alpha_{1i} =& -f_{1i}-\hat{\Delta}_{1i}+\dot{y}_{\mathrm{d}i}+\frac{k_{1i}z_{1i}}{2}(\chi_{i1}+\chi_{i2})\\ &+\frac{\iota_i}{2}(\chi_{i2}-\chi_{i1}).\end{aligned} \tag{33}$$

By rewriting Eq. (33) in vector form, we have

$$\begin{aligned}\boldsymbol{\alpha}_1 =& -\boldsymbol{f}_1-\hat{\boldsymbol{\Delta}}_1+\dot{\boldsymbol{y}}_{\mathrm{d}}\\ &+\frac{\boldsymbol{k}_1\boldsymbol{z}_1}{2}\mathrm{diag}(\chi_{i1}+\chi_{i2})+\frac{1}{2}\mathrm{diag}\left(\frac{\iota_i}{2}(\chi_{i2}-\chi_{i1})\right),\end{aligned} \tag{34}$$

where $\boldsymbol{k}_1=\mathrm{diag}\,(k_{11},k_{12},...,k_{1m})$ is the positive gain matrix and $\hat{\boldsymbol{\Delta}}_1$ is the estimate of $\boldsymbol{\Delta}_1$ presented in Section 3.1.

Substituting Eq. (33) into Eq. (32) produces

$$\dot{V}_1=-\sum_{i=1}^{n}k_{1i}\frac{z_{1i}^2}{1-z_{1i}^2}+\sum_{i=1}^{n}\frac{2z_{1i}z_{2i}}{(\chi_{i2}-\chi_{i1})(1-z_{1i}^2)}, \tag{35}$$

where the last term of Eq. (35) can be handled below.

Step 2: Define the following Lyapunov function candidate:

$$V_2=V_1+\frac{1}{2}\boldsymbol{z}_2^{\mathrm{T}}\boldsymbol{z}_2. \tag{36}$$

According to Eqs. (30) and (35), the time derivative of Eq. (36) is given as

$$\begin{aligned}\dot{V}_2 =&\dot{V}_1+\boldsymbol{z}_2^{\mathrm{T}}\dot{\boldsymbol{z}}_2\\ =&-\sum_{i=1}^{n}k_{1i}\frac{z_{1i}^2}{1-z_{1i}^2}+\sum_{i=1}^{n}\frac{2z_{1i}z_{2i}}{(\chi_{i2}-\chi_{i1})(1-z_{1i}^2)}\\ &+\boldsymbol{z}_2^{\mathrm{T}}(\boldsymbol{z}_3+\boldsymbol{\alpha}_2+\boldsymbol{f}_2+\boldsymbol{\Delta}_2-\dot{\boldsymbol{\alpha}}_1).\end{aligned} \tag{37}$$

The virtual control function $\boldsymbol{\alpha}_2$ can be designed as

$$\boldsymbol{\alpha}_2=-\boldsymbol{k}_2\boldsymbol{z}_2-\boldsymbol{f}_2-\hat{\boldsymbol{\Delta}}_2+\dot{\boldsymbol{\alpha}}_1-\boldsymbol{Q}, \tag{38}$$

where $\boldsymbol{\alpha}_1$ is as given in Eq. (34),

$$\boldsymbol{Q}=\begin{bmatrix}\frac{z_{11}}{(\chi_{12}-\chi_{11})(1-z_{11}^2)}\\ \frac{z_{12}}{(\chi_{22}-\chi_{21})(1-z_{12}^2)}\\ \vdots\\ \frac{z_{1m}}{(\chi_{m2}-\chi_{m1})(1-z_{1m}^2)}\end{bmatrix}, \tag{39}$$

$\boldsymbol{k}_2=\mathrm{diag}\,(k_{21},k_{22},...,k_{2m})$ is the positive gain matrix, and $\hat{\boldsymbol{\Delta}}_2$ is the estimate of $\boldsymbol{\Delta}_2$.

By substituting Eq. (38) into Eq. (37), we have

$$\dot{V}_2=-\sum_{i=1}^{n}k_{1i}\frac{z_{1i}^2}{1-z_{1i}^2}-\boldsymbol{z}_2^{\mathrm{T}}\boldsymbol{k}_2\boldsymbol{z}_2+\boldsymbol{z}_2^{\mathrm{T}}\boldsymbol{z}_3, \tag{40}$$

where the last term of Eq. (40) will be eliminated below.

Step i (i=3, 4, ..., $n-1$): Define the following Lyapunov function candidate:

$$V_i=V_{i-1}+\frac{1}{2}\boldsymbol{z}_i^{\mathrm{T}}\boldsymbol{z}_i. \tag{41}$$

According to Eqs. (30) and (40), the time derivative of Eq. (41) is given as

$$\begin{aligned}\dot{V}_i =&\dot{V}_{i-1}+\boldsymbol{z}_i^{\mathrm{T}}\dot{\boldsymbol{z}}_i\\ =&-\sum_{i=1}^{n}k_{1i}\frac{z_{1i}^2}{1-z_{1i}^2}-\sum_{j=2}^{i-1}\boldsymbol{z}_j^{\mathrm{T}}\boldsymbol{k}_j\boldsymbol{z}_j+\boldsymbol{z}_{i-1}^{\mathrm{T}}\boldsymbol{z}_i\\ &+\boldsymbol{z}_i^{\mathrm{T}}(\boldsymbol{z}_{i+1}+\boldsymbol{\alpha}_i+\boldsymbol{f}_i+\boldsymbol{\Delta}_i-\dot{\boldsymbol{\alpha}}_{i-1}).\end{aligned} \tag{42}$$

The virtual control function $\boldsymbol{\alpha}_i$ can be designed as

$$\boldsymbol{\alpha}_i=-\boldsymbol{z}_{i-1}-\boldsymbol{k}_i\boldsymbol{z}_i-\boldsymbol{f}_i-\hat{\boldsymbol{\Delta}}_i+\dot{\boldsymbol{\alpha}}_{i-1}, \tag{43}$$

where $\boldsymbol{k}_i=\mathrm{diag}\,(k_{i1},k_{i2},...,k_{im})$ is the positive gain matrix and $\hat{\boldsymbol{\Delta}}_i$ is the estimate of $\boldsymbol{\Delta}_i$.

Substituting Eq. (43) into Eq. (42) produces

$$\dot{V}_i=-\sum_{i=1}^{n}k_{1i}\frac{z_{1i}^2}{1-z_{1i}^2}-\sum_{j=2}^{i}\boldsymbol{z}_j^{\mathrm{T}}\boldsymbol{k}_j\boldsymbol{z}_j+\boldsymbol{z}_i^{\mathrm{T}}\boldsymbol{z}_{i+1}, \tag{44}$$

where the last term of Eq. (44) can be canceled below.

Step n: Define the following Lyapunov function candidate:

$$V_n=V_{n-1}+\frac{1}{2}\boldsymbol{z}_n^{\mathrm{T}}\boldsymbol{z}_n. \tag{45}$$

According to Eqs. (30) and (44), the time derivative of Eq. (45) is given as

$$\begin{aligned}\dot{V}_n =&\dot{V}_{n-1}+\boldsymbol{z}_n^{\mathrm{T}}\dot{\boldsymbol{z}}_n\\ =&-\sum_{i=1}^{n}k_{1i}\frac{z_{1i}^2}{1-z_{1i}^2}-\sum_{j=2}^{n-1}\boldsymbol{z}_j^{\mathrm{T}}\boldsymbol{k}_j\boldsymbol{z}_j+\boldsymbol{z}_{n-1}^{\mathrm{T}}\boldsymbol{z}_n\\ &+\boldsymbol{z}_n^{\mathrm{T}}(\boldsymbol{b}\boldsymbol{u}+\boldsymbol{f}_n+\boldsymbol{\Delta}_n-\dot{\boldsymbol{\alpha}}_{n-1}).\end{aligned}\tag{46}$$

In Section 2, we have mentioned that matrix $\boldsymbol{b}$ can be described as $\boldsymbol{b}=\boldsymbol{b}_1+\boldsymbol{b}_2$. Since matrix $\boldsymbol{b}_1$ is symmetric and $\boldsymbol{b}_2$ is skew-symmetric, for $\boldsymbol{z}_n\neq\boldsymbol{0}$, we denote $\varphi(t)=\dfrac{\boldsymbol{z}_n^{\mathrm{T}}\boldsymbol{b}_1\boldsymbol{z}_n}{\|\boldsymbol{z}_n\|^2}\neq 0$. If $\boldsymbol{z}_n=\boldsymbol{0}$, we define $\varphi(t)=\varphi_0>0$, where φ_0 is a constant satisfying $\lambda_{\min}(\boldsymbol{b}_1)\leq\varphi_0\leq\lambda_{\max}(\boldsymbol{b}_1)$. Then, we can obtain

$$\begin{cases}\boldsymbol{z}_n^{\mathrm{T}}\boldsymbol{b}_1\boldsymbol{z}_n=\varphi(t)\|\boldsymbol{z}_n\|^2,\\ \boldsymbol{z}_n^{\mathrm{T}}\boldsymbol{b}_2\boldsymbol{z}_n\equiv 0.\end{cases}\tag{47}$$

The control input $\boldsymbol{u}$ is designed as

$$\boldsymbol{u}=\frac{\boldsymbol{z}_n\boldsymbol{z}_n^{\mathrm{T}}}{\varphi\|\boldsymbol{z}_n\|^2}(-\boldsymbol{z}_{n-1}-\boldsymbol{k}_n\boldsymbol{z}_n-\boldsymbol{f}_n-\hat{\boldsymbol{\Delta}}_n+\dot{\boldsymbol{\alpha}}_{n-1}),\tag{48}$$

where $\boldsymbol{k}_n=\mathrm{diag}\,(k_{n1},k_{n2},...,k_{nm})$ is the positive gain matrix and $\hat{\boldsymbol{\Delta}}_n$ is the estimate of $\boldsymbol{\Delta}_n$.

Substituting Eq. (48) into Eq. (46), we can obtain

$$\begin{aligned}\dot{V}_n=&-\sum_{i=1}^{n}k_{1i}\frac{z_{1i}^2}{1-z_{1i}^2}-\sum_{j=2}^{n-1}\boldsymbol{z}_j^{\mathrm{T}}\boldsymbol{k}_j\boldsymbol{z}_j+\boldsymbol{z}_{n-1}^{\mathrm{T}}\boldsymbol{z}_n\\ &+\frac{\boldsymbol{z}_n^{\mathrm{T}}\boldsymbol{b}_1\boldsymbol{z}_n\boldsymbol{z}_n^{\mathrm{T}}}{\varphi\|\boldsymbol{z}_n\|^2}(-\boldsymbol{z}_{n-1}-\boldsymbol{k}_n\boldsymbol{z}_n-\boldsymbol{f}_n-\hat{\boldsymbol{\Delta}}_n+\dot{\boldsymbol{\alpha}}_{n-1})\\ &+\boldsymbol{z}_n^{\mathrm{T}}(\boldsymbol{f}_n+\boldsymbol{\Delta}_n-\dot{\boldsymbol{\alpha}}_{n-1})\\ =&-\sum_{i=1}^{n}k_{1i}\frac{z_{1i}^2}{1-z_{1i}^2}-\sum_{j=2}^{n}\boldsymbol{z}_j^{\mathrm{T}}\boldsymbol{k}_j\boldsymbol{z}_j.\end{aligned}\tag{49}$$

Then we can present the main result by the following theorem:

Theorem 2 Consider a class of high-order MIMO nonlinear systems (1) with system uncertainties and unknown external disturbances satisfying Assumptions 1–3. With the finite-time NN disturbance observer (14), adaptive law (16), and the proposed control law (48), the closed-loop system output can track the desired trajectory with all the signals bounded, and the transformed tracking error $\boldsymbol{z}_i$ is bounded. For any initial error satisfying the initial condition, the tracking error e_i can be guaranteed to be within the prescribed tracking performance.

Proof A Lyapunov function candidate is selected for the overall system as

$$\begin{aligned}V=&V_n+\sum_{i=1}^{n}V_{i0}\\ =&\frac{1}{2}\sum_{i=1}^{m}\ln\frac{1}{1-z_{1i}^2}+\frac{1}{2}\sum_{j=2}^{n}\boldsymbol{z}_j^{\mathrm{T}}\boldsymbol{z}_j\\ &+\frac{1}{2}\sum_{i=1}^{n}\left(\boldsymbol{s}_i^{\mathrm{T}}\boldsymbol{s}_i+\mathrm{tr}(\widetilde{\boldsymbol{W}}_i^{\mathrm{T}}\boldsymbol{\Gamma}_i^{-1}\widetilde{\boldsymbol{W}}_i)\right).\end{aligned}\tag{50}$$

According to inequality (20), Eqs. (49) and (50), and applying Lemma 2, the following inequality holds:

$$\begin{aligned}\dot{V}=&\dot{V}_n+\sum_{i=2}^{n}\dot{V}_{i0}\\ \leq&-\sum_{i=1}^{m}k_{1i}\frac{z_{1i}^2}{1-z_{1i}^2}-\sum_{j=2}^{n}\boldsymbol{z}_j^{\mathrm{T}}\boldsymbol{k}_j\boldsymbol{z}_j\\ &-\sum_{i=1}^{n}\left(\lambda_{\min}(\boldsymbol{k}_{0i})2^{\frac{a+b}{2b}}V_{i0}^{\frac{a+b}{2b}}+\eta_i\right)\\ \leq&-k_{1i}\sum_{i=1}^{m}\ln\frac{1}{1-z_{1i}^2}-\sum_{j=2}^{n}\boldsymbol{z}_j^{\mathrm{T}}\boldsymbol{k}_j\boldsymbol{z}_j\\ &-2\lambda_{\min}(\boldsymbol{k}_{0i})\sum_{i=1}^{n}V_{i0}+\sum_{i=1}^{n}\eta_i.\end{aligned}\tag{51}$$

Let

$$\begin{cases}\rho=\min\{4\lambda_{\min}(\boldsymbol{k}_{0i}),2k_{1i},2\lambda_{\min}(\boldsymbol{k}_j)\},\\ C=\sum_{k=1}^{n}\eta_k,\end{cases}\tag{52}$$

where i=1, 2, ..., m and j=2, 3, ..., n. Then inequality (51) can be rewritten as

$$\dot{V}\leq-\rho V+C.\tag{53}$$

To ensure $\rho>0$, the control parameters are chosen to satisfy

$$\lambda_{\min}(\boldsymbol{k}_{0i})>0,\ k_{1i}>0,\ \lambda_{\min}(\boldsymbol{k}_j)>0,\tag{54}$$

where i=1, 2, ..., m and j=2, 3, ..., n.

Thus, according to Lemma 4, the overall system is proven to be stable, and all the signals in the closed-loop system are bounded. The transformed tracking error z_{1i} can converge to the compact set described by

$$|z_{1i}|\leq\sqrt{1-\mathrm{e}^{-2(V(0)-C/\rho)}},\tag{55}$$

which means that the transformed tracking error z_{1i} is bounded in $(-1,1)$, satisfying condition (27). Therefore, the tracking error $\boldsymbol{e}$ can be guaranteed to be within the prescribed tracking performance. This completes the proof.

Remark 3 The whole control process could be divided into two stages. Considering Theorem 2, when $t<T_i$, the observation error and the tracking error are gradually converging but may not reach the desired bounds; when $t\geq T_i$, the observation error has converged to the range given in Eq. (22), and the tracking error is bounded. The control strategy is illustrated by a block diagram in Fig. 1.

4 Extension to high-order MIMO nonlinear systems with input saturation

In Section 3, we assume that the input signal is unconstrained. However, in the practical control process, especially for a mechanical system, the control input is always restricted. In this section, the observer-based tracking control of a high-order MIMO system with input saturation is considered.

With system (1), the control input variable $\boldsymbol{u}\in\mathbb{R}^m$ is redefined with the saturated condition, which is expressed as

$$\boldsymbol{u}_{\mathrm{s}}=\mathrm{sat}(\boldsymbol{v})=\begin{cases}\mathrm{sign}(\boldsymbol{v})u_{\mathrm{b}}, & \|\boldsymbol{v}\|\geq u_{\mathrm{b}},\\ \boldsymbol{v}, & \|\boldsymbol{v}\|<u_{\mathrm{b}},\end{cases}\tag{56}$$

where $\boldsymbol{u}_{\mathrm{s}}$ is the actual control input produced by saturated actuators, $\boldsymbol{v}=[v_1,v_2,...,v_m]^{\mathrm{T}}$ is the input signal generated by the processor to the actuators, and u_{b} is the known saturation bound.

According to He et al. (2015a), the original saturation signal has a sharp corner which is harmful to the system control, so an approximation function $\boldsymbol{h}(\boldsymbol{v})=[h(v_1),h(v_2),...,h(v_m)]^{\mathrm{T}}$ is raised to improve the saturation condition:

$$\boldsymbol{h}(\boldsymbol{v})=u_{\mathrm{b}}\tanh\left(\frac{\boldsymbol{v}}{u_{\mathrm{b}}}\right)=\boldsymbol{u}_{\mathrm{s}}\frac{\mathrm{e}^{\boldsymbol{v}/u_{\mathrm{b}}}-\mathrm{e}^{-\boldsymbol{v}/u_{\mathrm{b}}}}{\mathrm{e}^{\boldsymbol{v}/u_{\mathrm{b}}}+\mathrm{e}^{-\boldsymbol{v}/u_{\mathrm{b}}}}.\tag{57}$$

The control input signal in Eq. (56) can be transformed into

$$\boldsymbol{u}_{\mathrm{s}}=\mathrm{sat}(\boldsymbol{v})=\boldsymbol{h}(\boldsymbol{v})+\boldsymbol{g}(\boldsymbol{v}),\tag{58}$$

where $\boldsymbol{g}(\boldsymbol{v})=\mathrm{sat}(\boldsymbol{v})-\boldsymbol{h}(\boldsymbol{v})$ with the bound function:

$$\|\boldsymbol{g}(\boldsymbol{v})\|\leq u_{\mathrm{b}}(1-\tanh(1))=\overline{g}.\tag{59}$$

In this section, the input saturation will not affect the observer design process, so the disturbance observer is similar to the one designed in Section 3.1.

First, the transformed error dynamics coordinates with a full consideration of the input saturation (58) are described as

$$\begin{cases}\dot{\boldsymbol{z}}_1=[\dot{z}_{11},\dot{z}_{12},...,\dot{z}_{1m}]^{\mathrm{T}}\\ \quad=\mathrm{diag}\left(\frac{2}{\chi_{i2}-\chi_{i1}}\right)(\boldsymbol{x}_2+\boldsymbol{f}_1+\boldsymbol{\Delta}_1-\dot{\boldsymbol{y}}_{\mathrm{d}})-\iota_i,\\ \dot{\boldsymbol{z}}_j=\boldsymbol{x}_{j+1}+\boldsymbol{f}_j(\boldsymbol{x}_j)+\Delta\boldsymbol{f}_j(\boldsymbol{x}_j)+\boldsymbol{d}_j(t)-\dot{\boldsymbol{\alpha}}_{j-1},\\ \dot{\boldsymbol{z}}_n=\boldsymbol{b}\boldsymbol{u}_{\mathrm{s}}+\boldsymbol{f}_n(\boldsymbol{x}_n)+\Delta\boldsymbol{f}_n(\boldsymbol{x}_n)+\boldsymbol{d}_n(t)-\dot{\boldsymbol{\alpha}}_{n-1}-\dot{\boldsymbol{\gamma}},\\ e_i=y_i-y_{\mathrm{d}i}=\frac{1}{2}z_{1i}(\chi_{i2}-\chi_{i1})+(\chi_{i1}+\chi_{i2}),\end{cases}\tag{60}$$

where i=1, 2, ..., m, j=2, 3, ..., $n-1$, $\boldsymbol{\alpha}_k\in\mathbb{R}^m$ (k=1, 2, ..., $n-1$) is the virtual control function, and $\boldsymbol{\gamma}$ is

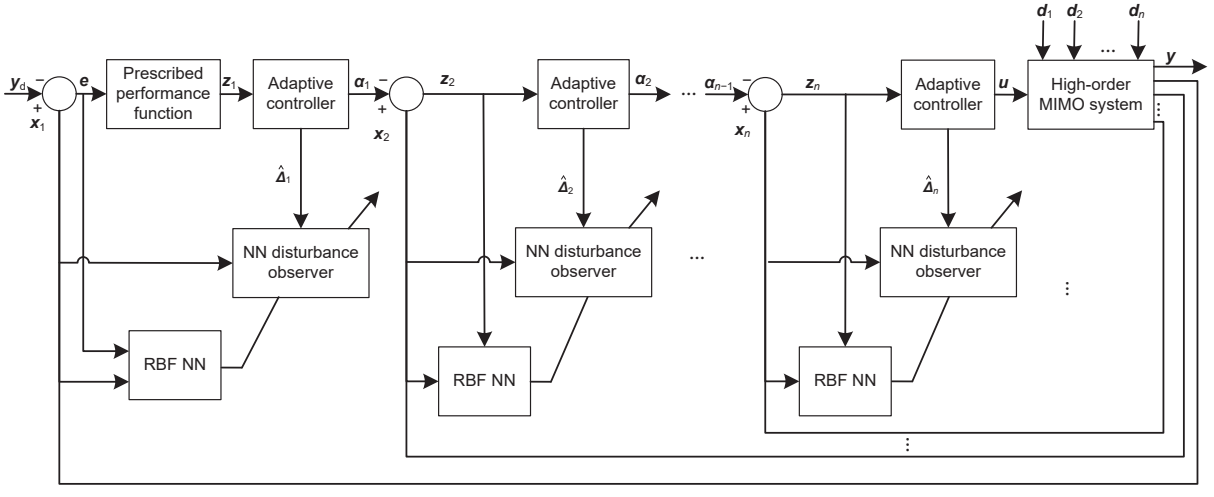

Fig. 1 Block diagram of the developed control strategy

a dynamic system defined as

$$\dot{\boldsymbol{\gamma}} = -\boldsymbol{\gamma} + \boldsymbol{b}(\boldsymbol{h}(\boldsymbol{v}) - \boldsymbol{v}). \tag{61}$$

Note that using the backstepping technique, the derivation of the control input $\dot{\boldsymbol{v}}$ is irrelevant to steps 1 to i (i=2, 3, ..., $n-1$); thus, the design procedure of these steps is similar to that in Section 3.3. The design process jumps directly to the last step involving $\boldsymbol{v}$.

Step n: Define the following Lyapunov function candidate:

$$V_n = V_{n-1} + \frac{1}{2}\boldsymbol{z}_n^{\mathrm{T}}\boldsymbol{z}_n. \tag{62}$$

According to Eq. (60), the time derivative of Eq. (62) is

$$\begin{aligned}\dot{V}_n =& \dot{V}_{n-1} + \boldsymbol{z}_n^{\mathrm{T}}\dot{\boldsymbol{z}}_n\\ =& -\sum_{i=1}^{n} k_{1i}\frac{z_{1i}^2}{1-z_{1i}^2} - \sum_{j=2}^{n-1}\boldsymbol{z}_j^{\mathrm{T}}\boldsymbol{k}_j\boldsymbol{z}_j + \boldsymbol{z}_{n-1}^{\mathrm{T}}\boldsymbol{z}_n\\ &+ \boldsymbol{z}_n^{\mathrm{T}}(\boldsymbol{b}\boldsymbol{u}_{\mathrm{s}} + \boldsymbol{f}_n + \boldsymbol{\Delta}_n - \dot{\boldsymbol{\alpha}}_{n-1} - \dot{\boldsymbol{\gamma}})\\ =& -\sum_{i=1}^{n} k_{1i}\frac{z_{1i}^2}{1-z_{1i}^2} - \sum_{j=2}^{n-1}\boldsymbol{z}_j^{\mathrm{T}}\boldsymbol{k}_j\boldsymbol{z}_j + \boldsymbol{z}_{n-1}^{\mathrm{T}}\boldsymbol{z}_n\\ &+ \boldsymbol{z}_n^{\mathrm{T}}(\boldsymbol{b}\boldsymbol{v} + \boldsymbol{f}_n + \boldsymbol{\Delta}_n - \dot{\boldsymbol{\alpha}}_{n-1} + \boldsymbol{\gamma} + \boldsymbol{b}\boldsymbol{g}(\boldsymbol{v})).\end{aligned} \tag{63}$$

Considering Eq. (47), the control input $\boldsymbol{v}$ can be designed as

$$\boldsymbol{v} = \frac{\boldsymbol{z}_n\boldsymbol{z}_n^{\mathrm{T}}}{\varphi\|\boldsymbol{z}_n\|^2}(-\boldsymbol{z}_{n-1} - \boldsymbol{k}_n\boldsymbol{z}_n - \boldsymbol{f}_n - \hat{\boldsymbol{\Delta}}_n + \dot{\boldsymbol{\alpha}}_{n-1} - \boldsymbol{\gamma}), \tag{64}$$

where parameter φ is defined similar to that in Eq. (47), $\boldsymbol{k}_n = \mathrm{diag}\,(k_{n1}, k_{n2}, ..., k_{nm})$ is the positive gain matrix, and $\hat{\boldsymbol{\Delta}}_n$ is the estimate of $\boldsymbol{\Delta}_n$.

By substituting Eq. (64) into Eq. (63), we can obtain

$$\begin{aligned}\dot{V}_n =& -\sum_{i=1}^{n} k_{1i}\frac{z_{1i}^2}{1-z_{1i}^2} - \sum_{j=2}^{n-1}\boldsymbol{z}_j^{\mathrm{T}}\boldsymbol{k}_j\boldsymbol{z}_j + \boldsymbol{z}_{n-1}^{\mathrm{T}}\boldsymbol{z}_n\\ &+ \boldsymbol{z}_n^{\mathrm{T}}\boldsymbol{b}_1\boldsymbol{v} + \boldsymbol{z}_n^{\mathrm{T}}(\boldsymbol{f}_n + \boldsymbol{\Delta}_n - \dot{\boldsymbol{\alpha}}_{n-1} + \boldsymbol{\gamma} + \boldsymbol{b}\boldsymbol{g}(\boldsymbol{v}))\\ =& -\sum_{i=1}^{n} k_{1i}\frac{z_{1i}^2}{1-z_{1i}^2} - \sum_{j=2}^{n-1}\boldsymbol{z}_j^{\mathrm{T}}\boldsymbol{k}_j\boldsymbol{z}_j + \boldsymbol{z}_{n-1}^{\mathrm{T}}\boldsymbol{z}_n\\ &+ \boldsymbol{z}_n^{\mathrm{T}}(-\boldsymbol{z}_{n-1} - \boldsymbol{k}_n\boldsymbol{z}_n - \boldsymbol{f}_n - \hat{\boldsymbol{\Delta}}_n + \dot{\boldsymbol{\alpha}}_{n-1} - \boldsymbol{\gamma})\\ &+ \boldsymbol{z}_n^{\mathrm{T}}(\boldsymbol{f}_n + \boldsymbol{\Delta}_n - \dot{\boldsymbol{\alpha}}_{n-1} + \boldsymbol{\gamma} + \boldsymbol{b}\boldsymbol{g}(\boldsymbol{v}))\\ =& -\sum_{i=1}^{n} k_{1i}\frac{z_{1i}^2}{1-z_{1i}^2} - \sum_{j=2}^{n}\boldsymbol{z}_j^{\mathrm{T}}\boldsymbol{k}_j\boldsymbol{z}_j + \boldsymbol{z}_n^{\mathrm{T}}\boldsymbol{b}\boldsymbol{g}(\boldsymbol{v}).\end{aligned} \tag{65}$$

Then the stability analysis of the designed controller is given in the following theorem:

Theorem 3 Consider a class of high-order uncertain MIMO nonlinear systems (1) with unknown external disturbance and input saturation satisfying Assumptions 1–3. With the finite-time NN disturbance observer (14), adaptive law (16), and the proposed control law (64), the closed-loop system output can track the desired trajectory $\boldsymbol{y}_{\mathrm{d}}$ with all signals bounded, and the transformed tracking error $\boldsymbol{z}_1$ is bounded. For any e_{i0} that satisfies the initial condition, the tracking error e_i can be guaranteed to be within the prescribed tracking performance.

Proof Similar to Section 3.3, the Lyapunov function candidate is selected as

$$\begin{aligned}V =& V_n + \sum_{i=1}^{n} V_{i0}\\ =& \frac{1}{2}\sum_{i=1}^{m}\ln\frac{1}{1-z_{1i}^2} + \frac{1}{2}\sum_{j=2}^{n}\boldsymbol{z}_j^{\mathrm{T}}\boldsymbol{z}_j\\ &+ \frac{1}{2}\sum_{i=1}^{n}\left(\boldsymbol{s}_i^{\mathrm{T}}\boldsymbol{s}_i + \mathrm{tr}(\widetilde{\boldsymbol{W}}_i^{\mathrm{T}}\boldsymbol{\Gamma}_i^{-1}\widetilde{\boldsymbol{W}}_i)\right).\end{aligned} \tag{66}$$

Substituting Eq. (65) and inequality (20) into Eq. (66) and applying Lemma 2, the following inequality holds:

$$\begin{aligned}\dot{V} =& \dot{V}_n + \sum_{i=2}^{n}\dot{V}_{i0}\\ \le& -\sum_{i=1}^{m} k_{1i}\frac{z_{1i}^2}{1-z_{1i}^2} - \sum_{j=2}^{n}\boldsymbol{z}_j^{\mathrm{T}}\boldsymbol{k}_j\boldsymbol{z}_j + \boldsymbol{z}_n^{\mathrm{T}}\boldsymbol{b}\boldsymbol{g}(\boldsymbol{v})\\ &- \sum_{i=1}^{n}\left(\lambda_{\min}(\boldsymbol{k}_{0i})2^{\frac{a+b}{2b}}V_{i0}^{\frac{a+b}{2b}} + \eta_i\right)\\ \le& -k_{1i}\sum_{i=1}^{m}\ln\frac{1}{1-z_{1i}^2} - \sum_{j=2}^{n}\boldsymbol{z}_j^{\mathrm{T}}\boldsymbol{k}_j\boldsymbol{z}_j + \overline{g}\|\boldsymbol{z}_n^{\mathrm{T}}\boldsymbol{b}\|\\ &- 2\lambda_{\min}(\boldsymbol{k}_{0i})\sum_{i=1}^{n}V_{i0} + \sum_{i=1}^{n}\eta_i.\end{aligned} \tag{67}$$

Similarly, let

$$\begin{cases}\rho_{\mathrm{s}} = \min\{4\lambda_{\min}(\boldsymbol{k}_{0i}), 2k_{1i}, 2\lambda_{\min}(\boldsymbol{k}_j)\},\\ C_{\mathrm{s}} = \sum_{k=1}^{n}\eta_k + \overline{g}\|\boldsymbol{z}_n^{\mathrm{T}}\boldsymbol{b}\|,\end{cases} \tag{68}$$

where i=1, 2, ..., m and j=2, 3, ..., n. Then inequality (67) can be rewritten as

$$\dot{V} \le -\rho_{\mathrm{s}}V + C_{\mathrm{s}}. \tag{69}$$

The control parameters are chosen to satisfy

$$\lambda_{\min}(\boldsymbol{k}_{0i})>0,\ k_{1i}>0,\ \lambda_{\min}(\boldsymbol{k}_j)>0, \tag{70}$$

where i=1, 2, ..., m and j=2, 3, ..., n.

Thus, by Lemma 4, the overall system is proven to be stable. According to inequality (69), we can see that all the signals in the closed-loop system are bounded. The transformed tracking error z_{1i} can converge to the compact set given as

$$|z_{1i}|\leq\sqrt{1-\mathrm{e}^{-2(V(0)-C_{\mathrm{s}}/\rho_{\mathrm{s}})}}, \tag{71}$$

which means that the transformed tracking error z_{1i} is bounded in $(-1,1)$. Therefore, the tracking error $\boldsymbol{e}$ can be guaranteed to be within the prescribed tracking performance with the existence of input saturation. This completes the proof.

5 Simulation results

In this section, the designed control method is used in the following quadrotor model to demonstrate its effectiveness. The dynamic model used in this study is an attitude dynamic model of the quadrotor in Wang XR et al. (2018), which is a classical uncertain MIMO system as follows:

$$\begin{cases}\ddot{\phi}(t)=\dfrac{I_y-I_z}{I_x}\dot{\theta}(t)\dot{\psi}(t)+\dfrac{l}{I_x}u_\phi+\dfrac{J_r}{I_x}\Omega\dot{\theta},\\ \ddot{\theta}(t)=\dfrac{I_z-I_x}{I_y}\dot{\psi}(t)\dot{\phi}(t)+\dfrac{l}{I_y}u_\theta+\dfrac{J_r}{I_y}\Omega\dot{\phi},\\ \ddot{\psi}(t)=\dfrac{I_x-I_y}{I_z}\dot{\phi}(t)\dot{\theta}(t)+\dfrac{1}{I_z}u_\psi,\end{cases} \tag{72}$$

where ϕ is the roll angle, θ is the pitch angle, ψ is the yaw angle, l is the distance from the center of gravity of the quadrotor to the center of each rotor, I_i ($i=x,\ y,\ z$) is the inertia of the quadrotor, J_r is the inertia of the propellers, Ω is the sum of the angular velocities of the motors, and u_ϕ, u_θ, and u_ψ are three input torques.

By analyzing model (72), we find it difficult to obtain an accurate value of the inertia parameters, which leads to model uncertainties. The quadrotor is disturbed by wind or other conditions during flight, so it is necessary to consider the external disturbance terms. The simulation also considers the existence and non-existence of input saturation, according to the various conditions of the actuator in practice. Therefore, system (72) can be rewritten as

$$\begin{cases}\dot{\boldsymbol{x}}_1=\boldsymbol{x}_2+\boldsymbol{f}_1(\boldsymbol{x}_1)+\Delta\boldsymbol{f}_1(\boldsymbol{x}_1)+\boldsymbol{d}_1(t),\\ \dot{\boldsymbol{x}}_2=\boldsymbol{B}\boldsymbol{u}+\boldsymbol{f}_2(\boldsymbol{x}_2)+\Delta\boldsymbol{f}_2(\boldsymbol{x}_2)+\boldsymbol{d}_2(t),\\ \boldsymbol{y}=\boldsymbol{x}_1,\end{cases} \tag{73}$$

where

$$\begin{cases}\boldsymbol{x}_1=[\phi,\theta,\psi],\\ \boldsymbol{x}_2=[\dot{\phi},\dot{\theta},\dot{\psi}],\\ \boldsymbol{f}_1=[0,0,0]^{\mathrm{T}},\\ \boldsymbol{B}=\mathrm{diag}\left(l/I_x,l/I_y,1/I_z\right),\\ \boldsymbol{u}=[u_\phi,u_\theta,u_\psi]^{\mathrm{T}},\\ \boldsymbol{f}_2(\boldsymbol{x}_2)=\left[\frac{I_y-I_z}{I_x}x_{22}x_{23},\frac{I_z-I_x}{I_y}x_{23}x_{21},\frac{I_x-I_y}{I_z}x_{21}x_{22}\right]^{\mathrm{T}}.\end{cases}$$

The terms for the total system disturbances to be estimated by disturbance observers are chosen as

$$\begin{cases}\Delta_1=0,\\ \boldsymbol{\Delta}_2=\begin{bmatrix}\dfrac{J_r}{I_x}\Omega x_{22}+d_{21}(t)\\ \dfrac{J_r}{I_y}\Omega x_{21}+d_{22}(t)\\ d_{23}(t)\end{bmatrix}.\end{cases} \tag{74}$$

The desired trajectories are designed as $\boldsymbol{y}_{\mathrm{d}}=[0.25\sin t,0.25\sin t,\sin t+0.5\sin(10t/7)]^{\mathrm{T}}$. The system parameters are chosen as $I_x=I_y=7.78\times10^{-3}$ kg/m^2, $I_z=1.44\times10^{-2}$ kg/m^2, $l=0.33$ m, $J_r=6\times10^{-3}$ kg/m^2. The external disturbances are given as $d_{21}=-0.1\cos(t/60)$, $d_{22}=0.05\sin(t/60)$, $d_{23}=-0.4\cos(t/50)$. The initial values of the system state are given as $\boldsymbol{x}_1=[4.5,4.5,9]^{\mathrm{T}}$, $\boldsymbol{x}_2=[0,0,0]^{\mathrm{T}}$.

The performance boundary function is shown as $\rho_i(t)=(\rho_{i0}-\rho_{i\infty})\mathrm{e}^{l_it}+\rho_{i\infty}$, and the prescribed parameters are chosen as $\rho_{10}=\rho_{20}=8$, $\rho_{30}=10$, $\rho_{i\infty}=0.5$, l_i=0.9, $\sigma_{ij}=1$ (i,j=1, 2, 3). The observer parameters are given as $\nu_i=1$, $\boldsymbol{k}_{0i}=\mathrm{diag}(0.01,0.01,0.1)$, $a_i=9$, $b_i=11$ (i=1, 2, 3). The parameters for the RBF NN in the observer are chosen as $\kappa_1=\kappa_2=0.1$, $\kappa_3=0.05$, $\Gamma_1=180$, $\Gamma_2=80$, $\Gamma_3=150$. The controller parameters are selected as $\boldsymbol{k}_1=\mathrm{diag}(60,42.5,64)$, $\boldsymbol{k}_2=\mathrm{diag}(600,595,420)$.

Case 1: Under the designed tracking control approach based on the NN disturbance observer, BLF, and the backstepping method, the simulation examples are presented in Figs. 2–7. The time responses of the Euler angles are depicted in Fig. 2, which indicates that the output can track the desired trajectories quite well under system uncertainties and

external disturbances. Additionally, the tracking errors and their constraints are shown in Fig. 3. It can be seen that by using the proposed scheme, the tracking errors can converge to a small neighborhood of the origin with predefined transient and steady-state bounds and that the prescribed tracking performance is attained.

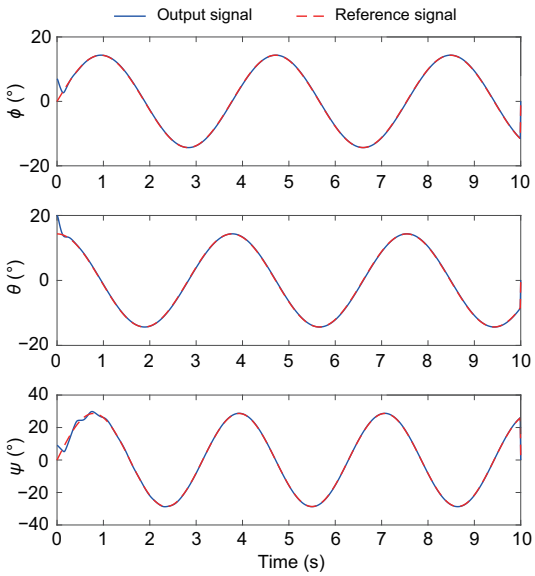

Fig. 2 Trajectories of the attitude angles of the quadrotor (blue line) along with the desired trajectory (red dashed line) under control input u (References to color refer to the online version of this figure)

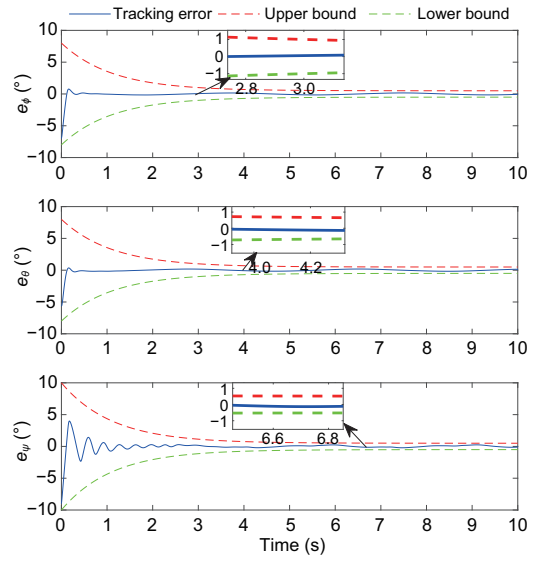

Fig. 3 Tracking error evolution with the prescribed performance under control input u (References to color refer to the online version of this figure)

The transformed tracking errors are presented in Fig. 4. Fig. 5 shows the convergence of the weight value of the NN. The estimates of the observers are given in Fig. 6, which illustrates that the uncertainties and disturbances can be handled well by the NN disturbance observer. It can be perceived in Fig. 7 that the input signals are non-chattering.

Case 2: In the simulation process, we find that the NN disturbance observer will introduce some

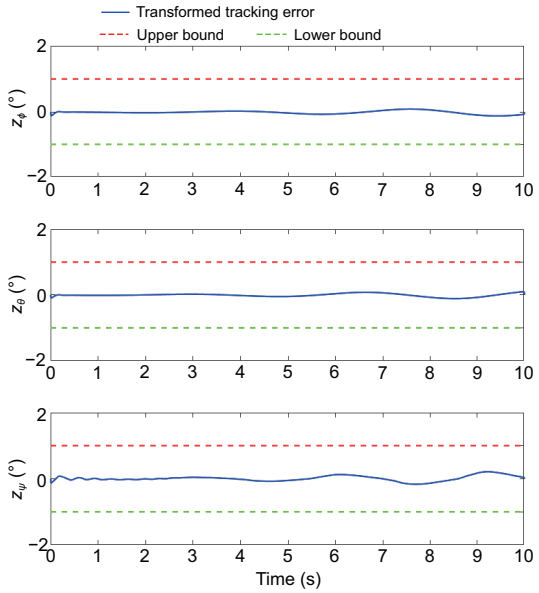

Fig. 4 Curves of the transformed tracking error $z(t)$ (References to color refer to the online version of this figure)

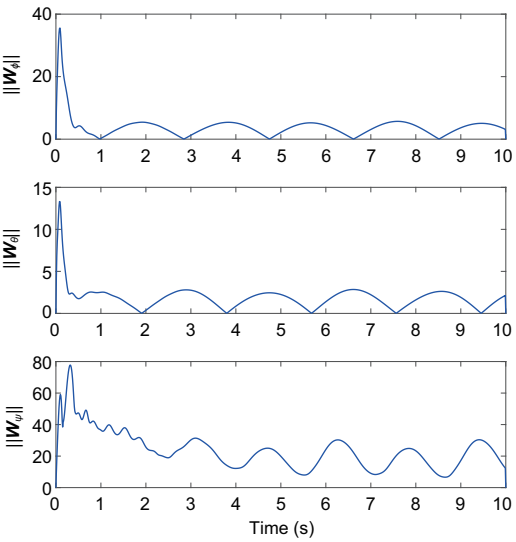

Fig. 5 Curves for the norm of the NN weight in the proposed NN disturbance observer

spikes to the control input, and these spikes exceed the operating range of the motors. Therefore, an input saturation condition is added to the control process and solved by controller (64).

The parameter for input saturation is set as $u_{\mathrm{b}} = 0.3$. According to Fig. 8, it can be concluded that the control inputs are restrained in the set range. The tracking performances under input saturation are shown in Figs. 9 and 10.

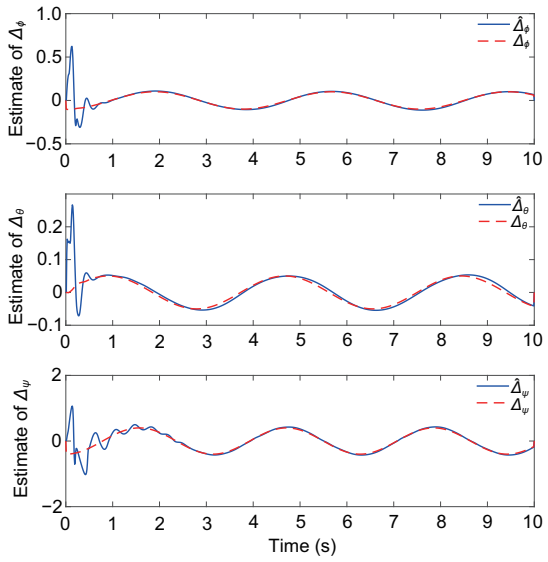

Fig. 6 Curves for disturbance estimation for $\boldsymbol{\Delta}(t)$ under the proposed NN disturbance observer

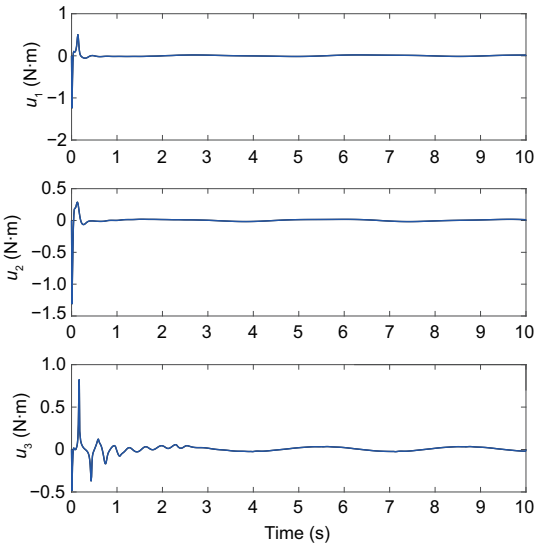

Fig. 7 Control demands u for attitude angles without input saturation

6 Conclusions

Observer-based adaptive tracking control has been investigated for a high-order MIMO nonlinear system with input saturation and prescribed tracking performance. In the control design, we have presented a novel NN disturbance observer to

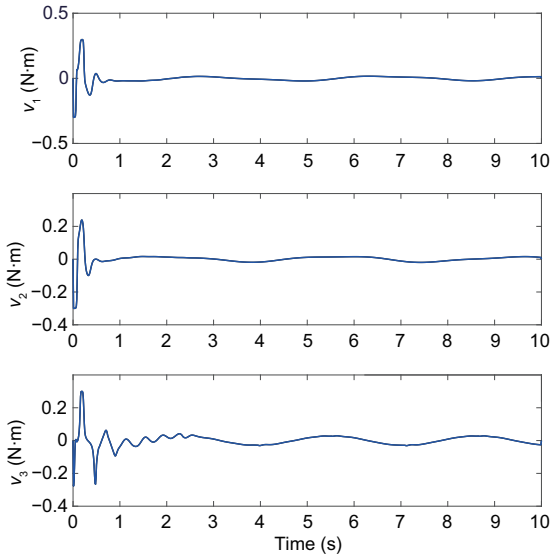

Fig. 8 Control demands v for attitude angles with input saturation

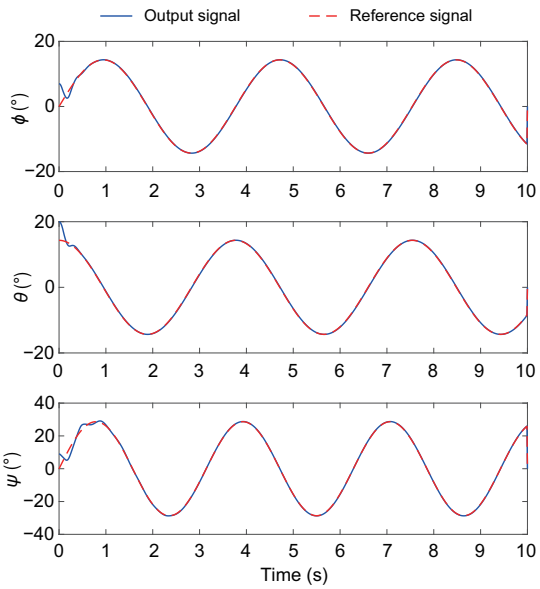

Fig. 9 Trajectories of the attitude angles of a quadrotor (blue line) along with the desired trajectory (red dashed line) under input v (References to color refer to the online version of this figure)

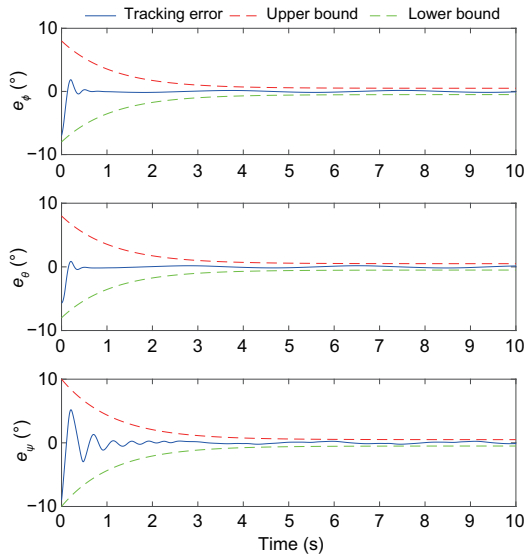

Fig. 10 Tracking error evolution with the prescribed performance under input v (References to color refer to the online version of this figure)

estimate the uncertainties and disturbances in finite time. Using the backstepping technique and BLF, an adaptive tracking control method has been proposed which could guarantee the prescribed performance of the tracking error and the boundedness of the closed-loop signals. Finally, the effectiveness of the designed scheme has been illustrated with extensive simulation results.

In the future, there is some meaningful work that needs to be conducted. The proposed method requires that the control coefficient matrix must be known. So, the design of an observer-based control strategy for a completely unknown system is still an open issue. Moreover, it is unclear whether the proposed result can be extended to nonlinear multi-agent systems.

Contributors

Xuerao WANG designed the research and drafted the manuscript. Qingling WANG helped organize the manuscript. Xuerao WANG and Changyin SUN revised and finalized the paper.

Compliance with ethics guidelines

Xuerao WANG, Qingling WANG, and Changyin SUN declare that they have no conflict of interest.

References

Bechlioulis CP, Rovithakis GA, 2008. Robust adaptive control of feedback linearizable MIMO nonlinear systems with prescribed performance. *IEEE Trans Autom Contr*, 53(9):2090-2099. https://doi.org/10.1109/TAC.2008.929402

Bechlioulis CP, Rovithakis GA, 2009. Adaptive control with guaranteed transient and steady state tracking error bounds for strict feedback systems. *Automatica*, 45(2):532-538. https://doi.org/10.1016/j.automatica.2008.08.012

Bechlioulis CP, Rovithakis GA, 2010. Prescribed performance adaptive control for multi-input multi-output affine in the control nonlinear systems. *IEEE Trans Autom Contr*, 55(5):1220-1226. https://doi.org/10.1109/TAC.2010.2042508

Bu XW, 2018. Guaranteeing prescribed output tracking performance for air-breathing hypersonic vehicles via non-affine back-stepping control design. *Nonl Dynam*, 91(1):525-538. https://doi.org/10.1007/s11071-017-3887-1

Chen M, Ge SS, Ren BB, 2011. Adaptive tracking control of uncertain MIMO nonlinear systems with input constraints. *Automatica*, 47(3):452-465. https://doi.org/10.1016/j.automatica.2011.01.025

Chen M, Mei R, Jiang B, 2013. Sliding mode control for a class of uncertain MIMO nonlinear systems with application to near-space vehicles. *Math Probl Eng*, 2013:180589. https://doi.org/10.1155/2013/180589

Chen WH, 2004. Disturbance observer based control for nonlinear systems. *IEEE/ASME Trans Mech*, 9(4):706-710. https://doi.org/10.1109/TMECH.2004.839034

Chen WH, Yang J, Guo L, et al., 2015. Disturbance-observer-based control and related methods—an overview. *IEEE Trans Ind Electron*, 63(2):1083-1095. https://doi.org/10.1109/TIE.2015.2478397

Chen XS, Yang J, Li SH, et al., 2009. Disturbance observer based multi-variable control of ball mill grinding circuits. *J Process Contr*, 19(7):1205-1213. https://doi.org/10.1016/j.jprocont.2009.02.004

Fan B, Yang QM, Jagannathan S, et al., 2017. Asymptotic tracking controller design for nonlinear systems with guaranteed performance. *IEEE Trans Cybern*, 48(7):2001-2011. https://doi.org/10.1109/TCYB.2017.2726039

Fu J, Ma RC, Chai TY, 2017. Adaptive finite-time stabilization of a class of uncertain nonlinear systems via logic-based switchings. *IEEE Trans Autom Contr*, 62(11):5998-6003. https://doi.org/10.1109/TAC.2017.2705287

Guo L, Chen WH, 2005. Disturbance attenuation and rejection for systems with nonlinearity via DOBC approach. *Int J Robust Nonl Contr*, 15(3):109-125. https://doi.org/10.1002/rnc.978

Guo XX, Yan WS, Cui RX, 2019. Integral reinforcement learning-based adaptive NN control for continuous-time nonlinear MIMO systems with unknown control directions. *IEEE Trans Syst Man Cybern Syst*, 50(11):4068-4077. https://doi.org/10.1109/TSMC.2019.2897221

Han SI, Lee JM, 2013. Improved prescribed performance constraint control for a strict feedback non-linear dynamic system. *IET Contr Theory Appl*, 7(14):1818-1827. https://doi.org/10.1049/iet-cta.2013.0181

He W, Dong YT, Sun CY, 2015a. Adaptive neural impedance control of a robotic manipulator with input saturation.

IEEE Trans Syst Man Cybern Syst, 46(3):334-344. https://doi.org/10.1109/TSMC.2015.2429555

He W, David AO, Yin Z, et al., 2015b. Neural network control of a robotic manipulator with input deadzone and output constraint. *IEEE Trans Syst Man Cybern Syst*, 46(6):759-770. https://doi.org/10.1109/TSMC.2015.2466194

Hu QL, Li B, Qi JT, 2014. Disturbance observer based finite-time attitude control for rigid spacecraft under input saturation. *Aerosp Sci Technol*, 39:13-21. https://doi.org/10.1016/j.ast.2014.08.009

Hu QL, Shao XD, Guo L, 2017. Adaptive fault-tolerant attitude tracking control of spacecraft with prescribed performance. *IEEE/ASME Trans Mech*, 23(1):331-341. https://doi.org/10.1109/TMECH.2017.2775626

Jin X, 2018. Adaptive decentralized finite-time output tracking control for MIMO interconnected nonlinear systems with output constraints and actuator faults. *Int J Robust Nonl Contr*, 28(5):1808-1829. https://doi.org/10.1002/rnc.3987

Lin LG, Xin M, 2020. Nonlinear control of two-wheeled robot based on novel analysis and design of SDRE scheme. *IEEE Trans Contr Syst Technol*, 28(3):1140-1148. https://doi.org/10.1109/TCST.2019.2899802

Lin XB, Yu Y, Sun CY, 2019a. A decoupling control for quadrotor UAV using dynamic surface control and sliding mode disturbance observer. *Nonl Dynam*, 97(1):781-795. https://doi.org/10.1007/s11071-019-05013-6

Lin XB, Yu Y, Sun CY, 2019b. Supplementary reinforcement learning controller designed for quadrotor UAVs. *IEEE Access*, 7:26422-26431. https://doi.org/10.1109/ACCESS.2019.2901295

Liu H, Xi JX, Zhong YS, 2017. Robust attitude stabilization for nonlinear quadrotor systems with uncertainties and delays. *IEEE Trans Ind Electron*, 64(7):5585-5594. https://doi.org/10.1109/TIE.2017.2674634

Liu J, Zhang YL, Yu Y, et al., 2019. Fixed-time event-triggered consensus for nonlinear multiagent systems without continuous communications. *IEEE Trans Syst Man Cybern Syst*, 49(11):2221-2229. https://doi.org/10.1109/TSMC.2018.2876334

Liu J, Zhang YL, Yu Y, et al., 2020. Fixed-time leader–follower consensus of networked nonlinear systems via event/self-triggered control. *IEEE Trans Neur Netw Learn Syst*, 31(11):5029-5037. https://doi.org/10.1109/TNNLS.2019.2957069

Liu J, Yu Y, He HB, et al., 2021. Team-triggered practical fixed-time consensus of double-integrator agents with uncertain disturbance. *IEEE Trans Cybern*, 51(6):3263-3272. https://doi.org/10.1109/TCYB.2020.2999199

Ouyang YC, Dong L, Xue L, et al., 2019. Adaptive control based on neural networks for an uncertain 2-DOF helicopter system with input deadzone and output constraints. *IEEE/CAA J Autom Sin*, 6(3):807-815. https://doi.org/10.1109/JAS.2019.1911495

Ouyang YC, Dong L, Sun CY, 2020. Critic learning-based control for robotic manipulators with prescribed constraints. *IEEE Trans Cybern*, online. https://doi.org/10.1109/TCYB.2020.3003550

Peng JZ, Ding S, Yang ZQ, et al., 2020. Adaptive neural impedance control for electrically driven robotic systems based on a neuro-adaptive observer. *Nonl Dynam*, 100(2):1359-1378. https://doi.org/10.1007/s11071-020-05569-8

Ren BB, Zhong QC, Chen JH, 2015. Robust control for a class of nonaffine nonlinear systems based on the uncertainty and disturbance estimator. *IEEE Trans Ind Electron*, 62(9):5881-5888. https://doi.org/10.1109/TIE.2015.2421884

Song YD, Huang XC, Wen CY, 2017. Robust adaptive fault-tolerant PID control of MIMO nonlinear systems with unknown control direction. *IEEE Trans Ind Electron*, 64(6):4876-4884. https://doi.org/10.1109/TIE.2017.2669891

Sui S, Tong SC, Li YM, 2015. Observer-based fuzzy adaptive prescribed performance tracking control for nonlinear stochastic systems with input saturation. *Neurocomputing*, 158:100-108. https://doi.org/10.1016/j.neucom.2015.01.063

Sun HB, Guo L, 2016. Neural network-based DOBC for a class of nonlinear systems with unmatched disturbances. *IEEE Trans Neur Netw Learn Syst*, 28(2):482-489. https://doi.org/10.1109/TNNLS.2015.2511450

Tee KP, Ge SS, Tay EH, 2009. Barrier Lyapunov functions for the control of output-constrained nonlinear systems. *Automatica*, 45(4):918-927. https://doi.org/10.1016/j.automatica.2008.11.017

Tong SC, Li YM, Shi P, 2012. Observer-based adaptive fuzzy backstepping output feedback control of uncertain MIMO pure-feedback nonlinear systems. *IEEE Trans Fuzzy Syst*, 20(4):771-785. https://doi.org/10.1109/TFUZZ.2012.2183604

Wang CC, Yang GH, 2018. Observer-based adaptive prescribed performance tracking control for nonlinear systems with unknown control direction and input saturation. *Neurocomputing*, 284:17-26. https://doi.org/10.1016/j.neucom.2018.01.023

Wang DD, Zong Q, Tian BL, et al., 2018. Neural network disturbance observer-based distributed finite-time formation tracking control for multiple unmanned helicopters. *ISA Trans*, 73:208-226. https://doi.org/10.1016/j.isatra.2017.12.011

Wang LY, Chai TY, Zhai LF, 2009. Neural-network-based terminal sliding-mode control of robotic manipulators including actuator dynamics. *IEEE Trans Ind Electron*, 56(9):3296-3304. https://doi.org/10.1109/TIE.2008.2011350

Wang QL, Sun CY, 2020. Adaptive consensus of multiagent systems with unknown high-frequency gain signs under directed graphs. *IEEE Trans Syst Man Cybern Syst*, 50(6):2181-2186. https://doi.org/10.1109/TSMC.2018.2810089

Wang XJ, Yin XH, Wu QH, et al., 2018. Disturbance observer based adaptive neural control of uncertain MIMO nonlinear systems with unmodeled dynamics. *Neurocomputing*, 313:247-258. https://doi.org/10.1016/j.neucom.2018.06.031

Wang XR, Sun CY, Lin XB, et al., 2018. Adaptive neural network control of a quadrotor with input delay. Proc Chinese Automation Congress, p.4095-4100. https://doi.org/10.1109/CAC.2018.8623376

Zhao Y, Yu SH, Lian J, 2020a. Anti-disturbance bumpless transfer control for switched systems with its application

to switched circuit model. *IEEE Trans Circ Syst II Expr Briefs*, 67(12):3177-3181.
https://doi.org/10.1109/TCSII.2020.2970068

Zhao Y, Zhao J, Fu J, et al., 2020b. Rate bumpless transfer control for switched linear systems with stability and its application to aero-engine control design. *IEEE Trans Ind Electron*, 67(6):4900-4910.
https://doi.org/10.1109/TIE.2019.2931222

Zheng ZW, Feroskhan M, 2017. Path following of a surface vessel with prescribed performance in the presence of input saturation and external disturbances. *IEEE/ASME Trans Mech*, 22(6):2564-2575.
https://doi.org/10.1109/TMECH.2017.2756110

Zhou Q, Shi P, Tian Y, et al., 2014. Approximation-based adaptive tracking control for MIMO nonlinear systems with input saturation. *IEEE Trans Cybern*, 45(10):2119-2128.
https://doi.org/10.1109/TCYB.2014.2365778

Zhu Z, Xia YQ, Fu MY, 2011. Attitude stabilization of rigid spacecraft with finite-time convergence. *Int J Robust Nonl Contr*, 21(6):686-702.
https://doi.org/10.1002/rnc.1624